IOP Conf. Series: Journal of Physics: Conf. Series **854** (2017) 012022 doi:10.1088/1742-6596/854/1/012022

Influence of the conservative rotor loads on the near wake of a wind turbine

I. Herráez[1], D. Micallef [2] and G.A.M. van Kuik[3]

[1] Dept. of Technology, University of Applied Sciences Emden/Leer, Constantiaplatz 4, 26723 Emden, Germany
[2] Dept. of Environmental Design, Faculty for the Build Environment, University of Malta, Msida MSD 2080, Malta
[3] Faculty of Aerospace Engineering, Technical University Delft, Kluyverweg 1, 2629HS, Delft, The Netherlands

E-mail: ivan.herraez@hs-emden-leer.de

Abstract. The presence of conservative forces on rotor blades is neglected in the blade element theory and all the numerical methods derived from it (like e.g. the blade element momentum theory and the actuator line technique). This might seem a reasonable simplification of the real flow of rotor blades, since conservative loads, by definition, do not contribute to the power conversion. However, conservative loads originating from the chordwise bound vorticity might affect the tip vortex trajectory, as we discussed in a previous work. In that work we also hypothesized that this effect, in turn, could influence the wake induction and correspondingly the rotor performance.

In the current work we extend a standard actuator line model in order to account for the conservative loads at the blade tip. This allows to isolate the influence of conservative forces from other effects. The comparison of numerical results with and without conservative loads enables to confirm qualitatively their relevance for the near wake and the rotor performance. However, an accurate quantitative assessment of the effect still remains out of reach due to the inherent uncertainty of the numerical model.

1. Introduction

The study of the fluid mechanics of propellers dates back to the 19^{th} century. Rankine [1] and Froude [2] settled the basis of the momentum theory explaining the origin of propeller thrust and torque from the momentum change in the fluid. This theory defines a limit to the efficiency of an ideal propeller but, due to the fact that this theory is one-dimensional, it does not provide any information about the required propeller geometry. On the contrary, the blade element theory, which is attributed to Drzewiecki [3], takes the rotor geometry into account by dividing each blade into a finite number of independent lifting surfaces (blade elements), although it does not define any limit to the propeller efficiency. This limitation is owed to the lack of consideration of the velocity induction of the propeller itself. In order to overcome the above mentioned drawbacks of both theories, Glauert [4] introduced the Blade Element Momentum (BEM) theory combining the momentum and the blade element theories. This theory has been successively improved over the years with many corrections that make it an essential tool for rotor design [5]. It is worth remarking that only fluid loads contributing to the power conversion

(i.e. non-conservative loads) are considered in BEM codes [6, 7]. The same applies to all other methods relying on the blade element theory. For example, the actuator line method (introduced by Sørensen and Shen [8]), replaces the momentum theory from the BEM method with the 3D Navier-Stokes equations for obtaining the induced velocities in the rotor plane. However, it also uses the blade element theory for computing the blade loads. Consequently, the actuator line (AL) method, which is gaining much attention in the field of wind farm simulations [9, 10, 11], also disregards the conservative loads. Conservative loads do not contribute to the power conversion and do not generate vorticity. Gravitational loads are a well known example of that type of load. However, aerodynamic loads on lifting surfaces, as rotor blades, might have a conservative component, too [12]. The origin of that load is the same as for the lift force: the bound circulation. At the root and tip of the blade, the bound circulation is deflected from the radial towards the chordwise direction before becoming free vorticity. The Kutta-Joukowsky load acting on the radial bound circulation gives rise to the lift force. In the same manner, the Kutta-Joukowsky load acting on the chordwise bound circulation gives rise to a force contained in a plane normal to the chord. Therefore, the load originating from the chordwise bound circulation can not contribute to the power conversion [12]. This article discusses the adequacy of neglecting this type of load in numerical models making use of the blade element theory.

Currently, rotor models that do not rely on the blade element theory are also widely-available (although they are more computationally expensive). For instance, Navier-Stokes models based on body-fitted grids have demonstrated to be very useful for the study of rotor aerodynamics [13, 14, 15, 16, 17]. Also vortex lattice models have proven to be reliable under attached flow conditions [18]. It is worth to recall that these types of models obtain the loads from the pressure field, which makes them capable of automatically considering the conservative loads (in opposition to the AL technique).

In Ref. [12] we used an AL, a vortex lattice and a body-fitted grid Navier-Stokes model for simulating the same wind turbine like in the present article. The models not relying on the blade element theory predicted a short inboard motion of the tip vortex just after release and before the wake expansion drove it outboard. This was in agreement with our experimental observations. Further experimental evidence of the same tip vortex behaviour is also available for other wind turbines [19, 20]. However, the AL model, which as mentioned above disregards the conservative load, was unable to predict that behaviour. This suggests a clear relationship between the tip vortex trajactory and the conservative load, what supports the hypothesis from previous analytical efforts. Furthermore, as we also hypothesized, the change in the tip vortex trajectory might influence the rotor performance. In order to analyse the validity of these hypothesis, in the current work we have extended an AL model for computing and applying automatically the conservative load at the tip. Hence, we aim at answering the following questions by comparing the baseline case (which only considers the non-conservative loads) with the extended model (which also considers the conservative load):

(i) Is it possible to modify the tip vortex trajectory of an actuator line model by considering the conservative load? In other words, is it possible to corroborate numerically by means of an enhanced actuator line model that the inboard motion of the tip vortex is a direct consequence of the conservative load at the blade tip?

(ii) If the previous question is answered affirmatively, is the influence of the mentioned effect on the rotor performance appreciable?

Section 2 introduces the numerical models that we use in our study. In §3 we first verify the reliability of the models and then compare the results of the simulations with and without conservative loads. This allows us to clarify what is the effect of the conservative loads. Finally, in §4 we present the main conclusions of this work in relation to our initial research questions.

2. Methods

2.1. Modelled wind turbine rotor

In this work we use the same experimental results as in our previous work [12] for verification purposes. Correspondingly, our study is based on the so called TUDelft-B wind turbine. The two-bladed rotor has a diameter of 2 meters. The blades are twisted and tapered. They make use of the DU96-W-180 airfoil type along the whole span except at the connection to the hub, where the blade section becomes cylindrical. The blade tip is not pointed but rectangular. The wind turbine is operated at its nominal conditions (tip speed ratio $\lambda = 7$). In the experiment the tip vortex trajectory was tracked by means of particle image velocimetry (PIV). Further details about the wind turbine and the experimental set-up can be found in Ref. [20, 21, 22, 23].

2.2. Numerical model

2.2.1. Navier-Stokes solver The simulations have been carried out with the open source toolbox OpenFOAM, which consists of a set of C++ libraries for solving partial differential equations [24]. All the computations are of the type Large Eddy Simulation (LES) and make use of a standard Smagorinsky sub-grid scale eddy viscosity model [25] for modelling the eddies of smaller size than the grid elements. The standard Smagorinky constant was set to $C_s = 0.168$, in accordance to the recommendations for isotropic turbulence [26, 27]. The discretization of the governing equations was based on the finite volume method. The time was discretized with a second order backward scheme. For the convective and diffusive terms we used second order linear upwind and linear limited differencing schemes, respectively. The pressure-velocity coupling was accomplished by means of the so called PIMPLE algorithm [24], which merges the PISO [28] and SIMPLE [29] algorithms.

2.2.2. Baseline actuator line model Our implementation of an actuator line (AL) model in OpenFOAM is based on the AL from the SOWFA package [30], which in turn is based on the original formulation proposed by Sørensen and Shen [8]. In this kind of model the actual geometry of each blade is substituted by a body force distributed along a line. In order to compute the body force, the actuator line is discretized into a finite number of blade elements. The user must predefine the blade geometry (spanwise distributions of chord and twist) as well as the aerodynamic characteristics of each blade element as a function of the angle of attack (AoA). Then, the AoA and the local lift $\boldsymbol{F_l}$ and drag $\boldsymbol{F_d}$ forces can be obtained iteratively from the above mentioned predefined data and the velocity field computed by the Navier-Stokes solver. In order to avoid numerical instabilities when applying the actuator line loading to the fluid, a gaussian smearing function is used for converting the point loads of each blade element into volumetric loads. The load applied to the fluid $\boldsymbol{f}$ was computed as:

$$\boldsymbol{f} = \frac{(\boldsymbol{F_l} + \boldsymbol{F_d})}{\epsilon^3 \pi^{3/2}} exp[-(r/\epsilon)^2] \tag{1}$$

where r is the distance between grid points and blade elements and ϵ represents a regularization parameter. Previous studies have shown a high dependency of the predicted power on the ϵ parameter. Therefore, in §3.1 we assess the sensitivity of our model to this parameter.
The hub is usually neglected in simulations based on the AL. As a consequence, an unrealistic jet appears along the centerline of the rotor. In order to overcome this issue, we modelled the nacelle as a permeable disk area, as described e.g. by Wu and Porte-Agél [31]. The force applied by the hub to the fluid is:

$$\boldsymbol{F_{hub}} = -\frac{1}{2}\rho \boldsymbol{u}_{\boldsymbol{\infty}}^2 A_{hub} C_{D_{hub}} \tag{2}$$

where u_∞ is the undisturbed velocity upstream of the hub, A_{hub} is the hub area and $C_{D_{hub}}$ is the hub drag coefficient. In our simulations we assumed $C_{D_{hub}} = 0.85$, as Ref. [31] suggests.

The wake induction on the rotor plane is automatically taken into account by the AL and there is no need for considering any correction for the finite number of blades (like e.g. the one proposed by Prandtl [4]). However, the AL disregards the pressure equalization between the pressure and suction sides of the blade. In order to overcome this limitation, we used the correction model developed by Shen *et al.* [32] for accounting for this effect on actuator models (in accordance to the recommendations of Sørensen [33], Chapt. 8.7). The correction model applies the following function to the 2D airfoil data:

$$F_1 = \frac{2}{\pi} cos^{-1}\left[exp\left(-g\frac{B(R-r)}{2rsin\phi}\right)\right] \tag{3}$$

where B is the number of blades, R is the blade radius, r is the local radial position, ϕ is the flow angle and g is the function

$$g = exp\left(-0.125\left(\frac{B\Omega R}{U_\infty} - 21\right)\right) + 0.1 \tag{4}$$

where Ω is the rotational speed and U_∞ is the freestream velocity.

The numerical domain consisted of a square cylinder with a length of 22R and a width of 20R, in accordance to the recommendations of Troldborg [9]. The rotor was placed at a distance of 10R from the inlet. The greatest cell density was concentrated around the rotor. In that region, which has the width 1.6R and the length 4R, the cell size is R/50. Outside that region the grid is progressively stretched towards the outer boundaries. It is worth to recall that a grid resolution with the cell size R/30 in the rotor region is usually considered to be enough for AL simulations [34, 8]. The reason why a finer resolution was used in our case was to capture the tip vortex trajectory as accurately as possible. For the same reason, 60 blade elements were used for modelling the blade in spite of the fact that 20 elements are usually considered to be enough [35]. Ivanell *et al.* [36] documented that in actuator line simulations the tip vortex is released slightly inboard of the tip. In our experience, this problem is related to the size of the blade elements in that region. Jin [37] also showed that increasing the blade element density at the tip is a computationally efficient manner of improving the simulation accuracy. Therefore, apart from having a relatively large number of elements, the spacing between elements in our simulation follows a stretching function that allows the element density to increase from the hub towards the blade tip. As a consequence, the blade elements at the tip are smaller than the cells themselves. This is advantageous for azimuthal positions at which only a tiny fraction of a cell is covered by the very tip of the blade.

A Dirichlet boundary condition was used for the wind speed at the inlet and for the pressure at the outlet. A Neumann condition was set for the pressure at the inlet and for the wind speed at the outlet. At the lateral boundaries of the domain, both the wind speed and the pressure were set to Neumann conditions.

2.2.3. Enhanced actuator line model The enhanced AL model only differs from the baseline model in the consideration of the conservative load at the blade tip. As we described in our previous work [12], the origin of the conservative force is the Kutta-Joukowski load acting on the chordwise bound circulation Γ_{chord}, which is defined as the circulation around a contour normal to the blade chord (see e.g. figure 5 from Ref. [12]). Hence, the normal $\mathscr{N}$ and radial $\mathscr{R}$ components of the conservative load are computed as:

$$\mathscr{N} = \rho \cdot V_{radial} \cdot \Gamma_{chord} \cdot c \tag{5}$$

$$\mathscr{R} = \rho \cdot V_{axial} \cdot \Gamma_{chord} \cdot c \tag{6}$$

where ρ is the fluid density, V_{radial} and V_{axial} are the radial and axial components of the relative velocity, respectively, and c is the chord length. Γ_{chord} is concentrated at the tip (see figures 7 and 9 from Ref. [12] , where the chordwise vorticity and circulation are shown), so $\mathscr{N}$ and $\mathscr{R}$ are applied as body forces only at the last blade element.

In order to obtain Γ_{chord} at the tip for applying the conservative load at the last blade element, we need to compute first the radial bound circulation along the span as

$$\Gamma_{radial}(r) = \frac{F_l(r)}{\rho \cdot V_{rel}(r)} \tag{7}$$

where F_l and V_{rel} are the sectional lift force and the relative wind speed, respectively. Γ_{radial} is computed for every single blade element. Once the magnitude of the maximum Γ_{radial} along the span is known, it can be used for estimating Γ_{chord} at the tip after assuming conservation of circulation. This assumption implies that Γ_{radial} is transformed into Γ_{chord} at the tip just before being converted into the tip vortex itself:

$$\Gamma_{chord} = z \cdot max(\Gamma_{radial}(r)) \tag{8}$$

where z is an engineering factor between 0 and 1 accounting for the fact, that a fraction of the maximum circulation is released as trailing circulation along the blade span before reaching the tip. We assume $z = 0.75$, since as figure 9 from Ref. [12] shows, that is approximately the normalized strength of the chordwise circulation (with respect to the maximum circulation) at the tip (assumed to be the last 2% of the blade length). In other words, 0.25 of the maximum bound circulation is released approximately from r/R = 0.8 (the radial position of maximum bound circulation) to 0.98 of the blade span. It should be however remarked that this assumption is just a best guess and it should be tuned in the future with more experiments and/or simulations. Furthermore, we expect this factor to be highly dependent on the blade geometry and the operating tip speed ratio.

3. Results

3.1. Verification of the baseline numerical model

It is well known that the accuracy of AL models highly depends on the regularization parameter ϵ. As Ivanell *et al.* [36] reported, ϵ must be as small as possible in order to avoid influencing the wake structure with the Gaussian smearing of the body force. However, the ratio $\epsilon/\Delta x$ (where Δx is the cell size in the rotor plane) can not be too small if numerical instabilities are to be avoided. Therefore, in order to achieve a small ϵ and resolve accurately the tip vortex, we chose in the first place a mesh that clearly exceeds the usual requirements of actuator line simulations (see §2.2.2). The power obtained from the simulations is used for analysing the sensitivity of the numerical model to the the ratio $\epsilon/\Delta x$ (see figure 1). The best consistency with the experiment (power overprediction of just 3%) is achieved with $\epsilon/\Delta x = 2$ (i.e. $\epsilon = R/25$). Troldborg [9] also suggested the same ratio as the best compromise between simulation accuracy and stability. For smaller values of $\epsilon/\Delta x$ the simulation was too unstable. Therefore, we chose to use $\epsilon/\Delta x = 2$ for both the baseline and enhanced models of our study.

As we explained in §2.2.3, the axial and radial velocity components are required for computing the conservative load that acts on the chordwise vorticity. Figure 2 shows those velocity components at the rotor plane as predicted by two different models: the current baseline AL model and the RANS model with body-fitted mesh that was validated in Ref. [12].

In spite of the fact that modelling a 3D blade by means of a 1D line is a strong simplification, the agreement between the AL and the body-fitted RANS model is in general good for both the axial and radial velocity components. However, a shift can be seen in the azimuthal position of the region with high radial velocity close to the blade tip. This implies that the radial velocity

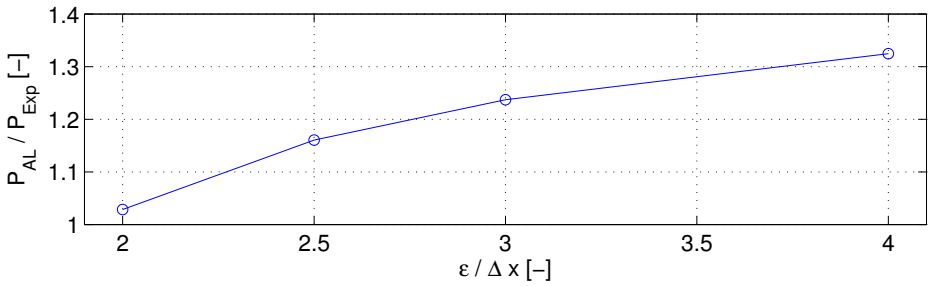

Figure 1. Sensitivity of the computed power from the baseline actuator model (normalized with the experimental results) to the ratio between the regularization parameter ϵ and the cell length Δx.

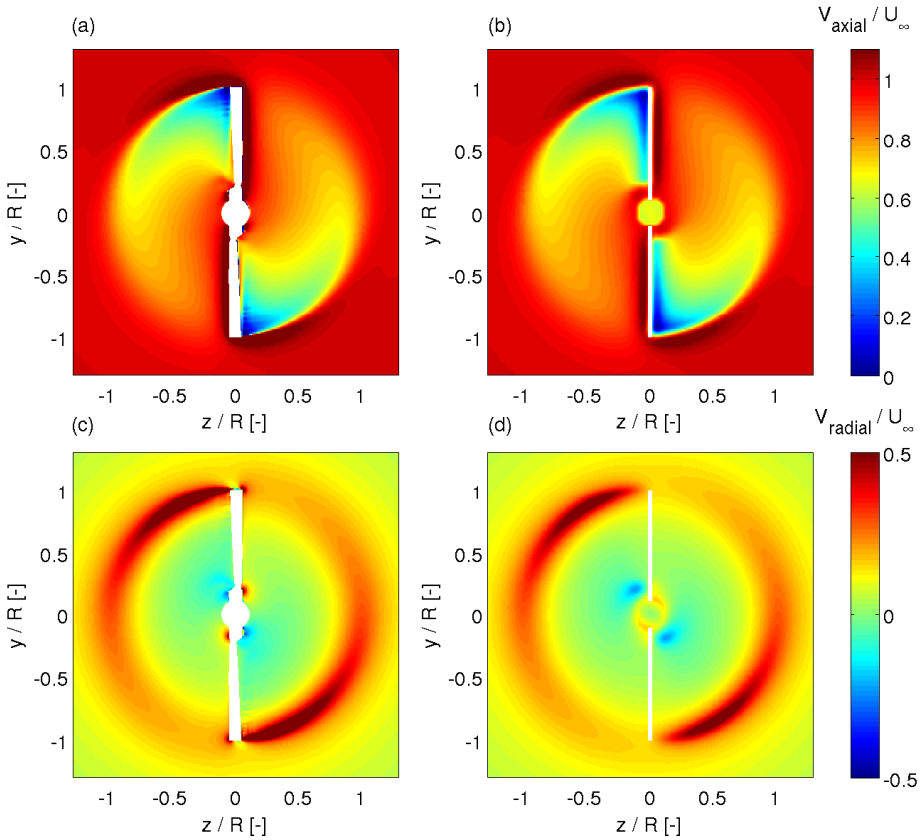

Figure 2. Velocity at the rotor plane: (a) V_{axial} from the body-fitted RANS simulation, (b) V_{axial} from the baseline AL-LES simulation, c) V_{radial} from the body-fitted RANS simulation and (d) V_{radial} from the baseline AL-LES simulation. The white surface in the results from the body-fitted RANS simulation represents the intersection of the rotor plane with the blades and nacelle. The white lines in the results from the AL-LES simulation represent the actuator lines.

	Body-fitted RANS	$AL_{baseline}$	$AL_{enhanced}$
$\mathscr{N}$	1.2	0	0.03
$\mathscr{R}$	1.2	0	1.2

Table 1. Normal and radial loads ($\mathscr{N}$ and $\mathscr{R}$, respectively) at the tip, as a percentage of the blade thrust. The body-fitted RANS results were obtained from the model presented in our previous work [12] and they were calculated by surface pressure integration. The enhanced AL model differs from the baseline model just in the consideration of the conservative loads attributed to chordwise vorticity.

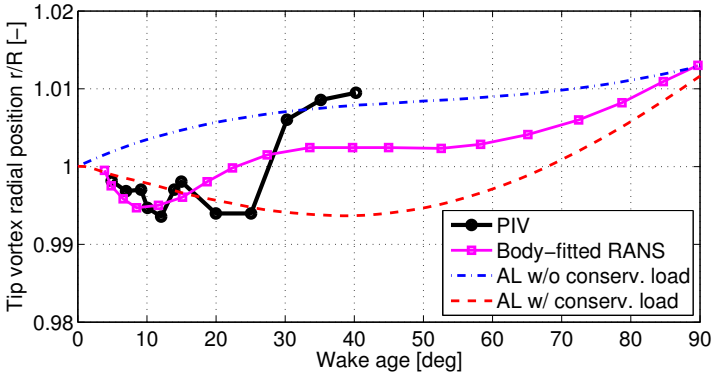

Figure 3. Radial position of the tip vortex as a function of the wake age. Experimental (Ref. [22]) and numerical results from different simulation models are compared.

at the tip of the baseline actuator line is strongly underpredicted. The same happens with the enhanced actuator line model (not shown in the figure, since differences in this regard with respect to baseline are negligible). The underprediction of the radial velocity component leads to a severe underestimation of the conservative load $\mathscr{N}$ (see equation 5), as represented in table 1. However, the radial component $\mathscr{R}$ is accurately predicted thanks to the good estimation of the axial velocity component.

3.2. Influence of the conservative load on the tip vortex trajectory

The λ_2 criteria [38] has been used for identifying the location of the vortex core at each azimuthal position. Figure 3 shows the vortex trajectory obtained from the experiment and different numerical models. Our analysis focuses on the AL-LES simulations, since the other results were already analysed in Ref. [12]. The AL-LES simulations without conservative load (labelled as *AL w/o conserv. load*) lead to the wake beginning to expand directly after the tip vortex release. On the contrary, the AL-LES simulations with conservative load (labelled as *AL w/ conserv. load*) present an inboard motion of the tip vortex prior to the wake expansion (as it also occurs in the experiment, the body-fitted RANS and panel lattice simulations). Furthermore, the computed radial position of the tip vortex at its innermost location agrees well with the experiment and the body-fitted RANS simulations. This behaviour confirms that the radial conservative load $\mathscr{R}$ is responsible for the inboard motion of the tip vortex, as we estimated in Ref. [12]. However, the azimuthal angle at which the wake expansion begins is clearly delayed in the AL-LES simulation. The reason for this seems to be related to the above described strong underestimation of $\mathscr{N}$ (see table 1).

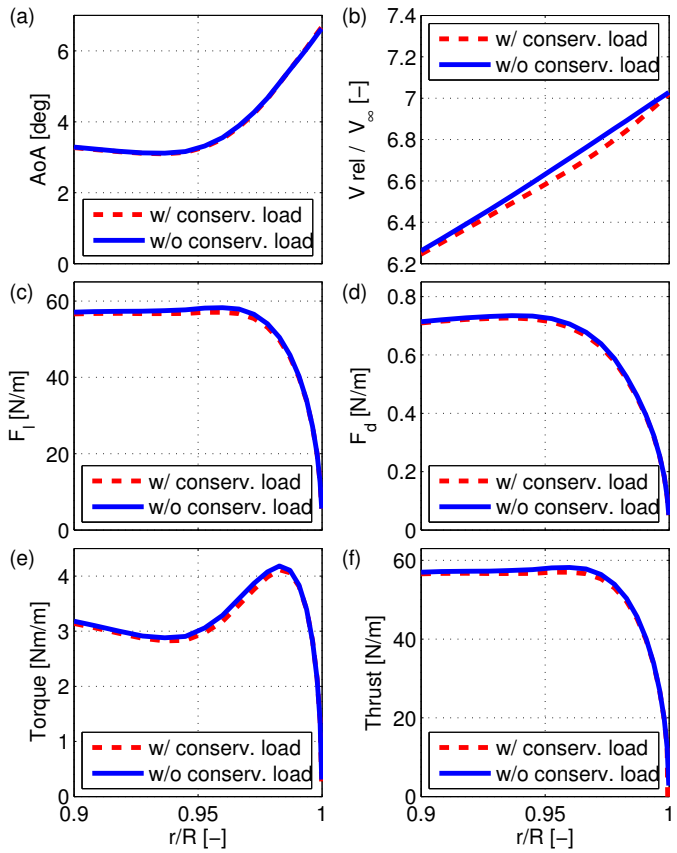

Figure 4. Influence of the conservative force on the spanwise distribution of (a) angle of attack AoA, (b) relative velocity V_{rel}, (c) sectional lift force F_l, (d) sectional drag force F_d, (e) sectional torque and (f) sectional thrust.

3.3. Influence of the conservative load on the rotor performance

In this section we aim at analysing if the influence of the conservative force on the tip vortex trajectory plays a role on the rotor performance. Figure 4-a shows the AoA in the tip region. No significant difference between the results with and without conservative force can be seen. This implies that the lift and drag force coefficients (C_l and C_d) do not change. However, the relative wind speed (figure 4-b), which is defined as $V_{rel} = \sqrt{V_x^2 + V_\theta^2}$, is slightly affected by the change in the vortex trajectory. Correspondingly, the lift and drag forces F_l and F_d are also influenced (figures 4-c and 4-d, respectively). This, in turn has a small but distinguishable effect on the driving torque and the thrust (figures 4-e and 4-f, respectively). Integrating the torque over the last 10% of the blade gives a difference of the torque at the tip with and without conservative load of approx. 2%. The total power of the turbine is reduced by approx. 1%. Hence, considering the conservative load contributes to mitigate the slight power overprediction of the simulation as compared to the experiment (see figure 1). This indicates that the conservative loads play an indirect, modest role on the rotor performance.

4. Conclusions

The use of an enhanced actuator line model capable of turning on and off the conservative load at the blade tip enabled studying the influence of the mentioned load on the aerodynamic performance and the near wake of a wind turbine. The model relates the maximum circulation along the span to the chordwise circulation at the tip by means of a factor z, which accounts for the trailing circulation. In order to estimate the value of that factor body-fitted CFD simulations (or experimental results with high spatial resolution) can be used. We expect our estimation of the mentioned parameter not to be valid for other turbines because of its high dependency on the blade geometry and the tip speed ratio. Once the chordwise vorticity at the tip is known, computing the conservative load is straightforward by means of the Kutta-Joukowski theorem.

The model allowed to corroborate that the conservative load can influence the tip vortex trajectory. Furthermore, it has been shown that this change might have a very small but non negligible impact on the rotor performance. However, quantifying this high order effect with sufficient accuracy is still not feasible because of the inherent uncertainty of the numerical model. Further research in this direction might be relevant for the development of physically-sound tip losses corrections models.

References

[1] W. J. M. Rankine. On the mechanical principles of the action of propellers. *Transactions Institute of Naval Architects*, 6:1339, 1865.
[2] R.E. Froude. On the part played in propulsion by differences of fluid pressure. *Transactions Institute of Naval Architects*, 30:390405, 1889.
[3] S. Drzewiecki. *Bulletin de L'Association Technique Maritime, Paris*, 1892.
[4] H. Glauert. The general momentum theory. In W.F. Durand, editor, *Aerodynamic Theory*, volume IV. Division L. Springer, 1935. Reprinted 1963 Dover.
[5] M. L. Hansen and H. Aagaard Madsen. Review paper on wind turbine aerodynamics. *Journal of Fluids Engineering*, 133(11):114001–114001–12, 2011.
[6] G. A. M. van Kuik, J. N. Sørensen, and V. L. Okulov. Rotor theories by Professor Joukowsky: Momentum theories. *Progress in Aerospace Sciences*, 73:1–18, 2015.
[7] V L Okulov, J N Sørensen, and D H Wood. The rotor theories by Professor Joukowsky: Vortex theories. *Progress in Aerospace Sciences*, pages 19–46, 2015.
[8] J. N. Sørensen and W. Z. Shen. Numerical modelling of wind turbine wakes. *Journal of Fluids Engineering*, 124(2):393–399, 2002.
[9] N. Troldborg. *Actuator Line Modeling of Wind Turbine Wakes*. PhD thesis, Technical University of Denmark, 2008.
[10] M. Shives and C. Crawford. Mesh and load distribution requirements for actuator line CFD simulations. *Wind Energy*, 16(8):1183–1196, 2013.
[11] K. Nilsson, W. Z. Shen, J. N. Sørensen, S. P. Breton, and S. Ivanell. Validation of the actuator line method using near wake measurements of the MEXICO rotor. *Wind Energy*, 18(3):499–514, 2015.
[12] G. A. M. van Kuik, D. Micallef, I. Herráez, A. H. van Zuijlen, and D. Ragni. The role of conservative forces in rotor aerodynamics. *Journal of Fluid Mechanics*, 750:284–315, 7 2014.
[13] N. N. Sørensen, J. A. Michelsen, and S. Schreck. Navier-Stokes predictions of the NREL phase vi rotor in the NASA ames 80 ft 120 ft wind tunnel. *Wind Energy*, 5(2-3):151–169, 2002.
[14] A. Bechmann, N. N. Sørensen, and F. Zahle. CFD simulations of the MEXICO rotor. *Wind Energy*, 14(5):677–689, 2011.
[15] I. Herráez, B. Stoevesandt, and J. Peinke. Insight into rotational effects on a wind turbine blade using Navier-Stokes computations. *Energies*, 7(10):6798, 2014.
[16] I. Herráez, B. Akay, G. J. W. van Bussel, J. Peinke, and B. Stoevesandt. Detailed analysis of the blade root flow of a horizontal axis wind turbine. *Wind Energy Science*, 1(2):89–100, 2016.
[17] N. N. Sørensen, A. Bechmann, P. E. Réthoré, and F. Zahle. Near wake Reynolds-averaged Navier-Stokes predictions of the wake behind the MEXICO rotor in axial and yawed flow conditions. *Wind Energy*, 17(1):75–86, 2014.
[18] D. Micallef, G. van Bussel, C. S. Ferreira, and T. Sant. An investigation of radial velocities for a horizontal axis wind turbine in axial and yawed flows. *Wind Energy*, 16(4):529–544, 2013.
[19] J. Xiao, J. Wu, L. Chen, and Z. Shi. Particle image velocimetry (PIV) measurements of tip vortex wake structure of wind turbine. *Appl. Math. Mech.*, 32(6):729–738, 2011.

[20] D. Micallef. *3D flows near a HAWT rotor: A dissection of blade and wake contributions*. PhD thesis, Delft University of Technology, 2012.
[21] D. Micallef, C.S. Ferreira, T. Sant, and G. J. W. van Bussel. Experimental and numerical investigation of tip vortex generation and evolution on horizontal axis wind turbines. *Wind Energy*, 19(8):1485–1501, 2016. we.1932.
[22] D. Micallef, B. Akay, C. S. Ferreira, T. Sant, and G. van Bussel. The origins of a wind turbine tip vortex. In *The Science of Making Torque from Wind 2012*, Oldenburg, Germany, October 2012.
[23] V. del Campo, D. Ragni, D. Micallef, B. Akay, F. J. Diez, and C. S. Ferreira. 3D load estimation on a horizontal axis wind turbine using SPIV. *Wind Energy*, 17(11):1645–1657, 2014.
[24] OpenFOAM. OpenFOAM: the open source CFD toolbox, 2015. Accessed: October 2015.
[25] J. Smagorinsky. General circulation experiments with the primitive equations. *Monthly Weather Review*, 91:99–164, 1963.
[26] D. K. Lilly. The representation of small–scale turbulence in numerical simulation experiments. In *Proc. IBM Scientific Computing Symposium on Environmental Sciences*, 1967.
[27] S. B. Pope. *Turbulent flows*. Cambridge University Press, 2000.
[28] R. I. Issa. Solution of the implicitly discretized fluid flow equations by operator-splitting. *Journal of Computational Physics*, 62:40–65, 1985.
[29] S. V. Patankar. *Numerical Heat Transfer and Fluid Flow*. Taylor & Francis, 1980.
[30] SOWFA. SOWFA: Simulator for wind farm applications, 2015. Accessed: October 2015.
[31] Y. T. Wu and F. Porte-Agél. Large-Eddy simulation of wind-turbine wakes: Evaluation of turbine parametrisations. *Boundary-Layer Meteorol*, 138:345–366, 12 2010.
[32] W. Z. Shen, J. N. Sørensen, and R. Mikkelsen. Tip loss correction for actuator/Navier-Stokes computations. *Journal of Solar Engineering*, 127:209–213, 2005.
[33] J. N. Sørensen. *General Momentum Theory for Horizontal Axis Wind Turbines*. Springer, 2015.
[34] W. Z. Shen, W. J. Zhu, and J. N. Sørensen. Actuator line/NavierStokes computations for the MEXICO rotor: comparison with detailed measurements. *Wind Energy*, 15(5):811–825, 2012.
[35] P. K. Jha, M. J. Churchfield, P. J. Moriarty, and S. Schmitz. Guidelines for volume force distributions within actuator line modeling of wind turbines on Large-Eddy Simulation-type grids. *J. Sol. Energy Eng.*, 136(3):031003–031003–11, 2014.
[36] S. Ivanell, J. N. Sørensen, R. Mikkelsen, and D. Henningson. Analysis of numerically generated wake structures. *Wind Energy*, 12(1):63–80, 2009.
[37] W. Jin. Numerical simulation of wind turbine wakes based on actuator line method in NEK5000. Master's thesis, KTH, Sweden, 2013.
[38] J Jeong and F Hussain. On the identification of a vortex. *Journal of Fluid Mechanics*, 285:69–94, 2 1995.